Application of the Normalized Surface Magnetic Source Model to a Blind Unexploded Ordnance Discrimination Test

Fridon Shubitidze [1], Juan Pablo Fernández [1], Irma Shamatava [1,2], Leonard R. Pasion [2], Benjamin E. Barrowes [1,3], and Kevin O'Neill [1,3]

[1] Thayer School of Engineering
Dartmouth College, Hanover, NH 03755-8000, USA
fridon.shubitidze@dartmouth.edu , jpfb@dartmouth.edu

[2] Sky Research, Inc.
112A-2386 East Mall, Vancouver, BC V6T 1Z3, Canada
irma.shamatava@dartmouth.edu , len.pasion@skyresearch.com

[3] USA ERDC Cold Regions Research and Engineering Laboratory
Hanover, NH 03755, USA
benjamin.e.barrowes@usace.army.mil, kevin.o'neill@erdc.usace.army.mil

***Abstract*—**The Normalized Surface Magnetic Source (NSMS) model is applied to unexploded ordnance (UXO) discrimination data collected at Camp Sibert, AL, with the EM63 electromagnetic induction sensor. The NSMS is a fast and accurate numerical forward model that represents an object's response using a set of equivalent magnetic dipoles distributed on a surrounding closed surface. As part of the discrimination process one must also determine the location and orientation of each buried target. This is achieved using a physics-based technique that assumes a target to be a dipole and extracts the location from the measured magnetic field vector and the scalar magnetic potential; the latter is reconstructed from field measurements by means of an auxiliary layer of magnetic charges. Once the object's location is estimated, the measured magnetic field is matched to NSMS predictions to determine the time-dependent amplitudes of the surface magnetic sources, which in turn can be used to generate classifying features. This paper shows the superior discrimination performance of the NSMS model.

***Index Terms*—**UXO, Camp Sibert tests, NSMS model, HAP method, discrimination, inversion.

I. INTRODUCTION

Unexploded ordnance (UXO) is a widespread, long-lasting, and deadly remnant of war and military practice that kills or maims hundreds of people worldwide each year. In the United States alone it is estimated that an area the size of the states of New Hampshire and Vermont put together—as many as 11 million acres of land—may be tainted with UXO, and that the eventual cost of cleaning up the contaminated land will reach the hundreds of billions of dollars [1],[2]. This is not because detecting UXO is difficult: low-frequency electromagnetic induction (EMI) sensors, on which we concentrate here, can easily penetrate the ground and find buried metal, and so can other methods like magnetometry or ground-penetrating radar. What makes the task of decontaminating UXO-polluted land so onerous and expensive is the inability of sensors to single out dangerous ordnance from the morass of innocuous items that usually surrounds them in the field; the latter can comprise smithereens from ordnance that did explode, high-metal-content geology, and anything else from nails to beer cans, all of which, in the absence of further information, must be treated as dangerous. The problem, then, consists of identifying hazardous items and

1054-4887 © 2010 ACES

distinguishing them from clutter as reliably and quickly as possible.

Much research is being presently conducted with the aim of making the UXO remediation process more efficient and economic. To support this effort by providing sound benchmarks, the Strategic Environmental Research and Development Program (SERDP) recently set up UXO discrimination blind tests at sites in Camp Sibert, a former U.S. Army facility near Gadsden, Alabama. Personnel from Sky Research, Inc. under the auspices of SERDP collected data at those test sites using the EM63, a time-domain EMI sensor produced by Geonics Ltd. [3]. The 216 targets buried at the sites include unexploded 4.2″ mortars, mortar explosion byproducts like base plates and bent half-shells, smaller shrapnel, and unrelated metallic clutter. In this paper we use those data to demonstrate the discrimination performance of a physically complete, fast, accurate, robust, and clutter-tolerant inverse-scattering approach called the Normalized Surface Magnetic Source (NSMS) model [4], which we present in Section II.

The signal scattered by an object depends both on the intrinsic features of the target (which the NSMS can encapsulate) and on its location and orientation relative to the sensor. Thus an essential step of the discrimination process is determining those extrinsic, observation-dependent factors as accurately as possible for each target. This nonlinear problem is usually attempted simultaneously with the characterization, an approach that often results in ill-posed and computationally expensive optimizations that take time and may yield unreliable answers. Here we bypass that difficulty by employing the physics-based field-potential (HAP) method [5], described in Section III, that pinpoints scatterers quickly and effectively.

The NSMS model and the HAP method ultimately stem from similar considerations. Scattered magnetic fields in the EMI regime are due to eddy currents or magnetic dipoles induced (and in some cases realigned) by the sensor and distributed nonuniformly inside the scatterers. Most of these sources tend to concentrate at some particular points, the so-called "scattered field singularities" (SFS); the study of the mathematical and physical properties of these singularities is part of the discipline known in the literature as "catastrophe theory" [6]. Recent work shows that under certain conditions the entire scatterer can be replaced with responding elementary sources placed at the SFS [7],[8].

In particular, the NSMS model replaces the scatterer—the UXO or piece of clutter, in this case—with a surrounding spheroid on which a set of radially oriented dipoles is distributed. The strengths of these dipoles are determined as those that best reproduce actual measurements; the composite dipole moment—here referred to as the "total NSMS"—varies significantly for different targets but is remarkably consistent for different specimens of the same object. In turn, the HAP technique assumes that the whole scatterer is a point dipole located at some SFS and finds its location and orientation by means of analytic expressions involving the dipole field and its associated scalar magnetic potential; to construct the latter from the former one distributes elementary sources on an auxiliary layer placed at a location intermediate between the sensor and the object and again finds the dipole moments by fitting measured data.

When combined, the two methods result in a powerful and efficient discrimination method for UXO. The precise location and orientation estimates given by the HAP allow an almost instantaneous determination of the time-dependent total NSMS. This can then be distilled further using an empirical decay law [9] whose fitting parameters can be mixed into discriminating features that tend to group in well-separated tight clusters, resulting in clear-cut classification. In the Camp Sibert blind test only one anomaly out of 216 was not identified correctly. In Section IV we discuss the procedure followed and the results obtained in this study, and in Section V we conclude.

II. THE NORMALIZED SURFACE SOURCE MODEL

The NSMS can be thought of as a generalization of the infinitesimal dipole model [9],[10],[11], with which it coincides in the limit. The dipole model postulates that for any given object it is possible to find a set of three orthonormal "body" axes such that a uniform primary field impinging along any of those directions induces a magnetization—and hence a dipole moment—parallel and linearly proportional

to it. A primary field $\mathbf{H}^{\mathrm{pr}}$ pointing along an arbitrary direction thus creates a dipole moment $\mathbf{m} = \bar{\bar{\mathbf{M}}} \cdot \mathbf{H}^{\mathrm{pr}}$, where the polarizability tensor $\bar{\bar{\mathbf{M}}}$ projects $\mathbf{H}^{\mathrm{pr}}$ onto the body system, finds the magnetization components there—this being the only step that depends on the object and not on the geometry—and synthesizes the dipole moment back in the global frame. The point dipole model is conceptually simple, fast, and reasonably powerful, and for that reason has been frequently used in discrimination studies [9],[12],[13]. However, its limitations become apparent when the target to be identified is heterogeneous, and thus composed of two or more mutually interacting sections, or when, as is usually the case in EMI measurements, the primary field established by the sensor varies appreciably over the dimensions of the target and strikes each region with a different intensity and direction. These problems can be addressed by substituting the single point dipole with an assembly of responding sources.

In the particular version of the NSMS used for the Camp Sibert test we distribute dipoles on a prolate spheroidal surface that surrounds the object of interest. By choosing a spheroid we simultaneously exploit the realism granted by its orientable elongated shape and the simplicity afforded by its azimuthal symmetry—a quality spheroids share with most UXO. We divide the spheroid S into subsurfaces (either patches or belts) and assign

$$\mathbf{H}^{\mathrm{sc}}(\mathbf{r}) = \oint_S \frac{M(s')}{4\pi R_{s'}^3}\left[\frac{3(\boldsymbol{\xi}_{s'}\cdot\mathbf{R}_{s'})\mathbf{R}_{s'}}{R_{s'}^2} - \boldsymbol{\xi}_{s'}\right] ds', \quad (1)$$

where $\mathbf{R}_{s'} = \mathbf{r} - \mathbf{r}_{s'}$ is a vector that points from the location $\mathbf{r}_{s'}$ of the s'-th infinitesimal patch on the spheroid to the observation point $\mathbf{r}$ and $\boldsymbol{\xi}_{s'}$ is the unit vector normal to the patch, which is most easily found in prolate spheroidal coordinates. All of these quantities clearly depend on the location and orientation of the spheroid relative to the sensor. The dipole directions are fixed by their locations on the spheroid, so to factor out the geometric particulars we set

$$M(s') = \Omega(s')\,[\boldsymbol{\xi}(s')\cdot\mathbf{H}^{\mathrm{pr}}(s')], \quad (2)$$

which defines a new normalized surface polarization distribution $\Omega(s')$. Such a distribution can be generated by spreading virtual positive magnetic charge over the exterior of an infinitesimally thin spheroidal shell and negative charge on its inner surface, resulting in a double layer. This configuration introduces the proper discontinuities in the tangential components of the magnetic flux density vector $\mathbf{B}$ at the boundary between two media but does not affect its normal component, keeping $\mathbf{B}$ divergence-free and the model consistent with the absence of free magnetic monopoles in nature.

By choosing a suitable quadrature scheme it is possible to transform Eq. (1) into the matrix-vector product $\mathbf{H}^{\mathrm{sc}} = \bar{\bar{\mathbf{Z}}} \cdot \Omega$. Each column of the scattering matrix $\bar{\bar{\mathbf{Z}}}$ corresponds to a different subsurface, and each row to a measurement point at which data are collected. The amplitude vector Ω can be determined directly, and with great speed and accuracy, by minimizing in a least-squares sense the difference between measured data and the predictions of Eq. (1) at a sufficient set of points for a known object-sensor configuration:

$$\min_{\Omega} \tfrac{1}{2}\left(\bar{\bar{\mathbf{Z}}} \cdot \tfrac{1}{2} - \mathbf{H}^{\mathrm{meas}}\right)^2, \quad (3)$$

whose solution is the normal equation

$$\tfrac{1}{2} = [\bar{\bar{\mathbf{Z}}}^{\mathrm{T}} \cdot \bar{\bar{\mathbf{Z}}}]^{-1}[\bar{\bar{\mathbf{Z}}}^{\mathrm{T}} \cdot \mathbf{H}^{\mathrm{meas}}]. \quad (4)$$

Once Ω is found one can define a "total" or "average" polarizability by integrating over the whole spheroid. The resulting quantity

$$Q = \oint_S \Omega(s')\, ds' \quad (5)$$

is a global magnetic capacitance of sorts. Different studies [4] have shown that, within reasonable limits, Q for a given object is invariant with respect to the constructs used for its determination: spheroid size and aspect ratio, measurement grid, object location or orientation, primary field, etc. It is thus intrinsic to the object and can be used, on its own or combined with other quantities, in discrimination processing, either within a "genuine" inversion procedure that uses Q itself as a discriminant or through a "pattern matching" method that compares measured fields to those stored in a library of known objects and

determines which known UXO has the catalogued source distribution that best reproduces the signal received by the survey sensor. Used in this way, the NSMS system is a faster forward model than other physically motivated models such as the standardized excitation approach (SEA) [14],[15] or the generalized SEA described in [16],[17].

The actual signal picked up by the sensor is more complicated than Eq. (1), since, in observance of Faraday's Law, it is the negative of the time derivative of the magnetic flux through the receiver coil. Thus it is necessary to perform an additional quadrature to incorporate the surface integral over the coil (and have Q absorb a minus sign). A deeper issue has to do with the time dependence of Q. Equations (1)–(4) are evaluated separately at each time gate and formally yield a "time-dependent" distribution $Q(t)$, even though in rigor the transient response must take into account the complete history of excitation and involve both the impulse response of the target and the waveform of the sensor. Still, it is reasonable to determine and use the amplitude $Q(t)$, even though it has no actual physical reality, because its manifestation is unique. Moreover, we are interested only in the field *outside* the targets, where it can be assumed that electromagnetic phenomena occur instantaneously. A thorough study of this problem, including detailed calculations of full time responses, can be found in Ref. [18].

III. A METHOD TO ESTIMATE THE LOCATION OF A BURIED OBJECT

Consider a point dipole located at $\mathbf{r}_d$ with a moment $\mathbf{m}$ that in general may be dependent on frequency or time. In the magnetoquasistatic regime that concerns us the dipole generates at the observation point $\mathbf{r}$ a field

$$\mathbf{H}(\mathbf{r}) = \frac{1}{4\pi R^3}\left[\frac{3(\mathbf{m}\cdot\mathbf{R})\mathbf{R}}{R^2} - \mathbf{m}\right], \tag{6}$$

where $\mathbf{R} = \mathbf{r} - \mathbf{r}_d$, which in turn can be derived from the scalar potential

$$\psi(\mathbf{r}) = \frac{\mathbf{m}\cdot\mathbf{R}}{4\pi R^3}. \tag{7}$$

A simple algebraic manipulation lets us find $\mathbf{r}_d$ in terms of $\mathbf{H}$ and ψ: take the dot product of $\mathbf{H}$ and $\mathbf{R}$ and use ψ to show that

$$\mathbf{H}\cdot\mathbf{R} = 2\frac{\mathbf{m}\cdot\mathbf{R}}{4\pi R^3} = 2\psi, \tag{8}$$

which can be cast as

$$\mathbf{H}\cdot\mathbf{r}_d = -2\psi + \mathbf{H}\cdot\mathbf{r}. \tag{9}$$

Given N observation points it is possible to find a least-squares estimate of the dipole location using

$$\begin{bmatrix} H_{x,1} & H_{y,1} & H_{z,1} \\ H_{x,2} & H_{y,2} & H_{z,2} \\ \vdots & & \\ H_{x,N} & H_{y,N} & H_{z,N} \end{bmatrix} \begin{bmatrix} x_d \\ y_d \\ z_d \end{bmatrix} = \begin{bmatrix} -2\psi_1 + \mathbf{H}_1\cdot\mathbf{r}_1 \\ -2\psi_2 + \mathbf{H}_2\cdot\mathbf{r}_2 \\ \vdots \\ -2\psi_N + \mathbf{H}_N\cdot\mathbf{r}_N \end{bmatrix} \tag{10}$$

since at every point i we know the location $\mathbf{r}_i$ of the sensor and the value $\mathbf{H}_i$ of the vector magnetic field. The only quantity not readily available is the scalar potential, but that can be reconstructed using a method similar to that from the preceding section. We assume that the scattered magnetic field is produced by a set of magnetic sources—charges, in this case—placed on a fictitious surface located just below the measurement points. The field is then

$$\mathbf{H}(\mathbf{r}_i) = \int \frac{q(s')}{4\pi}\frac{\mathbf{r}_i - \mathbf{r}_{s'}}{\left|\mathbf{r}_i - \mathbf{r}_{s'}\right|^3}\, ds', \tag{11}$$

to which corresponds a scalar potential

$$\psi(\mathbf{r}_i) = \int \frac{q(s')}{4\pi\left|\mathbf{r}_i - \mathbf{r}_{s'}\right|}\, ds'. \tag{12}$$

The positions $\mathbf{r}_{s'}$ of the sources are fixed and known by construction, so it remains to determine the charges $q(s')$. This is again achieved by minimizing the difference between model predictions and collected data $\mathbf{H}^{\text{meas}}$ at a set of known points. We use a quadrature scheme to turn Eq. (11) into a matrix-vector product and then determine

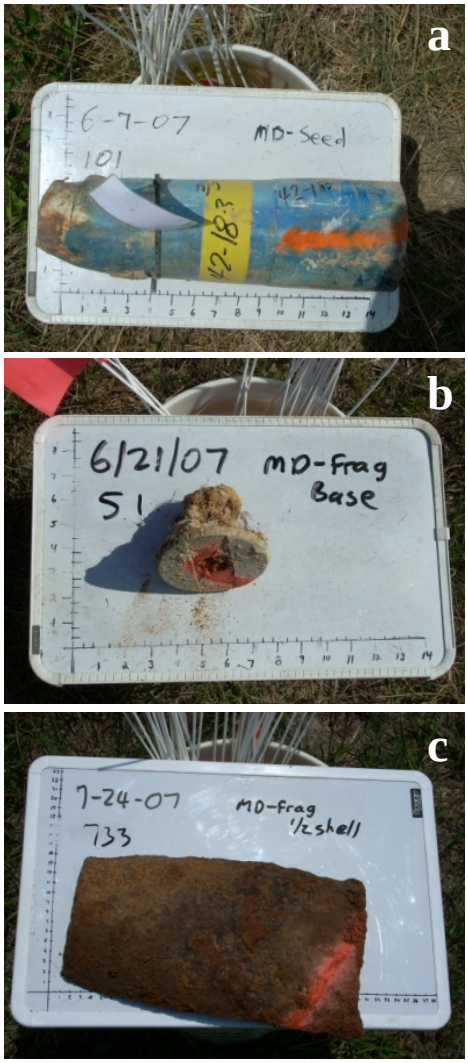

Fig. 1. Example items buried in the ground at the Camp Sibert plots: a) 4.2-inch mortar, b) base plate, c) partial mortar.

$$\min_{\mathbf{q}} \frac{1}{2} \left(\begin{bmatrix} \mathbf{Z}_x \\ \mathbf{Z}_y \\ \mathbf{Z}_z \end{bmatrix} \cdot \mathbf{q} - \begin{bmatrix} \mathbf{H}_x^{\text{meas}} \\ \mathbf{H}_y^{\text{meas}} \\ \mathbf{H}_z^{\text{meas}} \end{bmatrix} \right)^2 , \qquad (13)$$

where each matrix row corresponds to a different measurement point and each column to a subsurface of the underground virtual source layer. This method and its adaptation to monostatic sensors (like that used for the Camp Sibert test) are discussed in detail in Ref. [5].

IV. NUMERICAL RESULTS

The Camp Sibert blind-test data was collected over 216 cells, each of which was a square of side 5 m and contained one anomaly. There were three main kinds of targets: 4.2″ UXO, base plates, and partial mortars (Fig. 1), to which were added smaller shrapnel and non-UXO related scrap. We were given a set of calibration data for each type of object, which we used to build a catalog of expected total NSMS values.

The Geonics EM63 collects data over 26 time channels, with the first gate centered at 180 μs and the last at 25 ms. Approximately 700 data points were taken per time channel at each cell; the measurement locations for a typical cell (which in this particular case contained a mortar target) are shown as points in Fig. 2. The figure shows the scattered field values measured by the sensor (left column) and reconstructed by the combined procedure from the previous sections (right column), along with the absolute value of the difference between the two. The top row corresponds to the very first time gate and the bottom row depicts the 20th, centered at 7.65 ms. We see that the predictions agree well with the actual values. Our next task is to see whether these reasonable predictions are realizations of a sound model.

Initially we solved simultaneously for the total NSMS and the location and orientation of each anomaly using a Levenberg-Marquardt nonlinear least-squares optimization [19]. The results of that procedure are presented elsewhere [20]. As seen in that reference, it was difficult to categorize each target reliably because there tended to be a large uncertainty in the location. (To save time we performed the Levenberg-Marquardt search only once per target, so many of those optimizations may have reported finding a local minimum.) We obtained much better results by finding the locations and orientations of the targets using the HAP method and then characterizing the located objects using a 3D NSMS code. The inverted total NSMS strengths for all anomalies appear on Fig. 3. The figure also separates the curves corresponding to each of the major kinds of targets sought.

The total NSMS depends on the size, the geometry, and the material composition of the object it represents. Early time gates bring out the high-frequency response to the shutdown of the

exciting field; since the skin depth $\delta \propto f^{-1/2}$, the eddy currents in this range are superficial, and a large NSMS amplitude at early times correlates with large objects whose surface stretches wide. At late times, where the eddy currents have diffused completely into the object and low-frequency harmonics dominate, the EMI response relates to the metal content (volume) of the target. Thus a smaller but compact object like the base plate of Fig. 1(c) has a relatively weak early response that dies down slowly, while a large but thin, essentially hollow object like the partial mortar (bent half-shell) of Fig. 1(d) has an initially strong response that decays quickly. The unexploded 4.2″ mortar, being large and tightly packed, has a substantial early response that persists for a long time.

The previous considerations may be put on a more quantitative footing through discrimination features that summarize these characteristics (initial amplitude, time constant, etc.) for the different NSMS curves. To that end we employ an empirical power-law/exponential decay expression first proposed by Pasion and Oldenburg [9],

$$Q(t) = kt^{-\beta}e^{-\gamma t}, \tag{14}$$

where t is the time, k, β, and γ are fitting parameters, and $Q(t)$ is the total NSMS from Fig. 3. After investigating different combinations of k, β, and γ we found that the ratio of Q at the 15th time channel to Q at the first time channel, which involves a fixed combination of β and γ, showed good classification ability when plotted against k. Figure 4 depicts $Q(t_{15})/Q(t_1)$ versus k for all items. The results show a clear and robust clustering in this feature space that can result in dependable classification. In particular, we see that the values for the 4.2″ mortars are

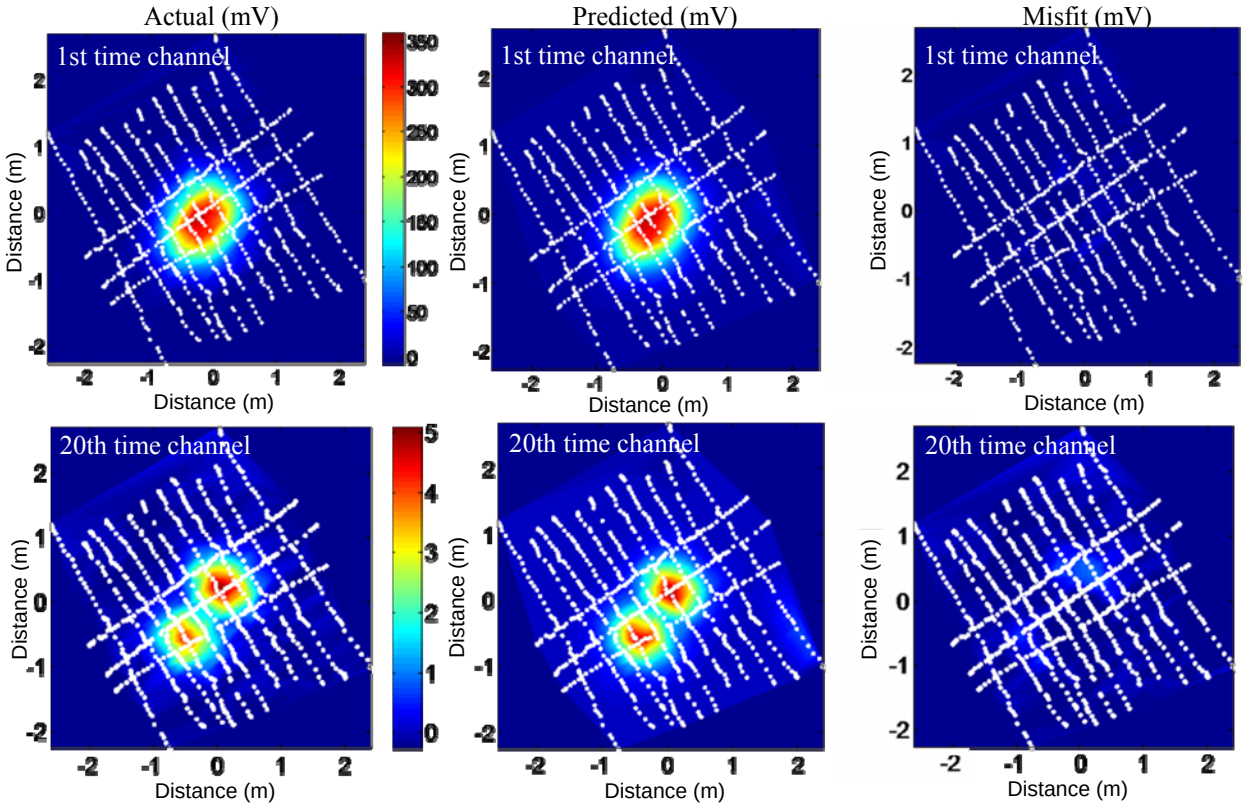

Fig. 2. EM63 data sets: near field distributions for a typical case, measured (left column), predicted (middle), and misfit (right). The white dots show the measurement points on the 5 m-by-5 m square plot. The first time channel (top row) is taken 80 μs after shutdown; the 20th (bottom) corresponds to 7.65 ms.

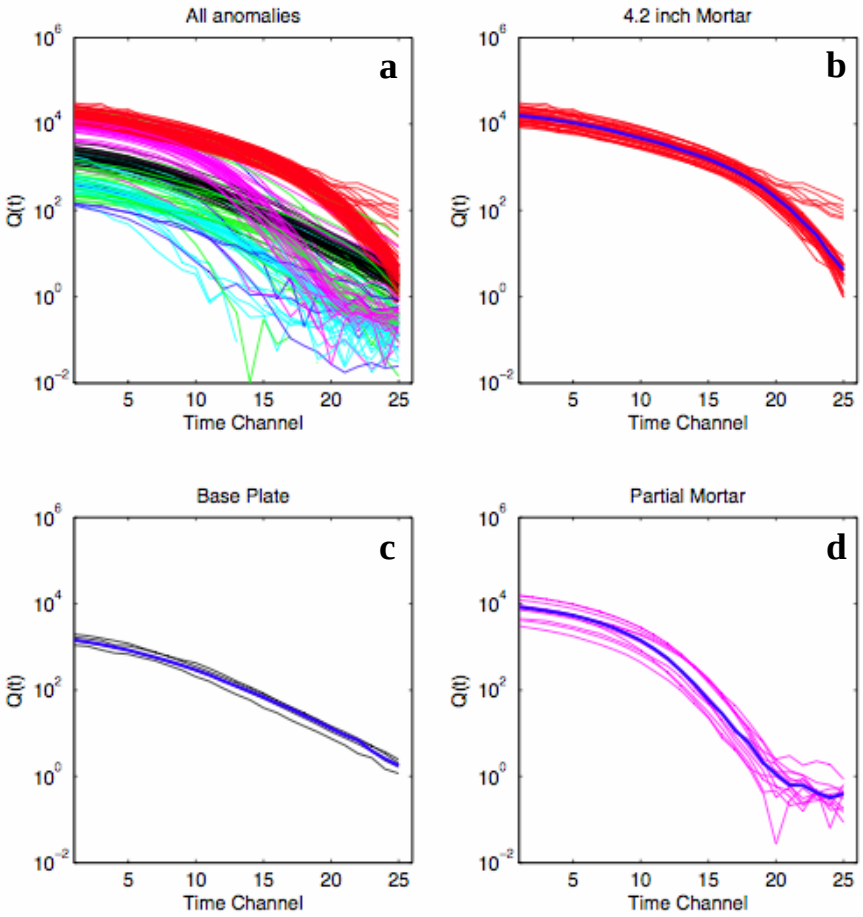

Fig. 3. Inverted total NSMS amplitudes for all anomalies (a) and classification results. The UXO (red, b) have a large spatial extent and thus a large initial amplitude, as do the partial mortars (bent hollow shells) (magenta, d). They are also packed tight and hence have a high metal concentration, just like the base plates (gray, c), resulting in a relatively slow time decay. The other objects are much smaller.

very well grouped and noticeably distinct from those of the base plates and the partial mortars. We knew the ground truth for 66 of the anomalies and used that information to make predictions for the other 150. Our combined NSMS/HAP method correctly identified all UXO and had only one false alarm. The resulting Receiver Operating Characteristic (ROC) curve, omitted here, is an almost perfect square.

The combination of $Q(t_{15})/Q(t_1)$ and k is a solid discriminator but not the only one available. It is possible to study directly the clustering of k, β, and γ in a 3D feature space or perform a similar analysis for the full $Q(t)$. We are in the process of implementing classification algorithms that do just that and will present the results in forthcoming reports.

V. CONCLUSION

In this paper we applied the NSMS model to the EM-63 Camp Sibert discrimination data sets. First the locations of the objects were inverted for by means of a very efficient and accurate dipole-inspired method; subsequently each anomaly was characterized at each time channel through its total NSMS strength. Classification features were selected and extracted for each object using the Pasion-Oldenburg decay law. Our study reveals that the ratio of an object's late response to its early response provides a good discrimination parameter when plotted against the Pasion-

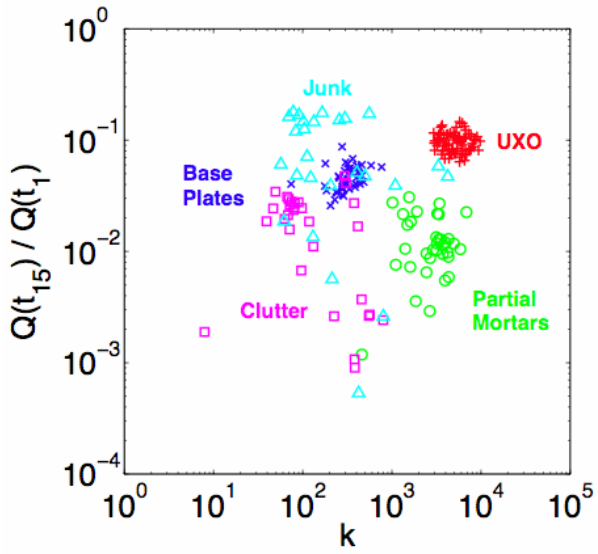

Fig. 4. The total NSMS ratio $Q(t_{15})/Q(t_1)$ becomes a robust classifier when plotted against the feature-space parameter k. The (red) crosses that correspond to the mortars are particularly well clustered and distinctly separate from the markers belonging to the other target types.

Oldenburg amplitude. These results, and those of other tests [21],[22], show that the NSMS/HAP combined procedure is capable of correctly singling out UXO from among munitions-related debris and other clutter, both natural and artificial, that always plagues former battlefields and proving grounds. It is thus a strong candidate to help solve the serious international problem of UXO proliferation.

ACKNOWLEDGEMENT

This work was supported by the Strategic Environmental Research and Development Program through grant # MM-1572.

REFERENCES

[1] B. Johnson *et al.*, "A research and development strategy for unexploded ordnance sensing," tech. rep. EMP-1, MIT Lincoln Lab, Lexington, MA, 1996.

[2] Federal Advisory Committee for the Development of Innovative Technologies, "Unexploded ordnance (UXO): An overview," https://www.denix.osd.mil, 1996.

[3] J. D. McNeill and M. Bosnar, "Application of TDEM techniques to metal detection and discrimination: a case history with the new Geonics EM-63 fully time-domain metal detector," tech. note TN-32, Geonics LTD, Mississauga, ON, 2000.

[4] F. Shubitidze, K. O'Neill, B. Barrowes, I. Shamatava, K. Sun, J. P. Fernández, and K. D. Paulsen, "Application of the normalized surface magnetic charge model to UXO discrimination in cases with overlapping signals," *J. Appl. Geophys.*, vol. 61, pp. 292–303, 2007.

[5] F. Shubitidze, D. Karkashadze, B. Barrowes, I. Shamatava, and K. O'Neill, "A new physics based approach for estimating a buried object's location, orientation and magnetic polarization for EMI data," *J. Environ. Eng. Geophys.*, vol. 13, pp. 115–130, 2008.

[6] V. I. Arnold, *Catastrophe Theory*, second edition, Springer, Berlin, 1986.

[7] A. G. Kyurkchan, B. Yu. Sternin, and V. E. Shatalov, "Singularities of continuation of wave fields," *Phys. Usp.*, vol. 31, pp. 1221–1242, 1996.

[8] R. Zaridze, G. Bit-Babik, K. Tavzarashvili, D. P. Economou, and N. K. Uzunoglu, "Wave field singularity aspects in large-size scatterers and inverse problems," *IEEE Trans. Antennas Propag.*, vol. 50, pp. 50–58, 2002.

[9] L. R. Pasion and D. W. Oldenburg, "A discrimination algorithm for UXO using time domain electromagnetics," *J. Environ. Eng. Geophys.*, vol. 6, pp. 91–102, 2001.

[10] J. Van Bladel, *Electromagnetic Fields*, first edition, McGraw-Hill, New York, 1964.

[11] F. S. Grant and G. F. West, *Interpretation Theory in Applied Geophysics*, McGraw-Hill, New York, 1965.

[12] T. H. Bell, B. J. Barrow, and J. T. Miller, "Subsurface discrimination using electromagnetic induction sensors," *IEEE Trans. Geosci. Remote Sens.*, vol. 39, pp. 1286–1293, 2001.

[13] Y. Zhang, L. Collins, H. Yu, C. E. Baum, and L. Carin, "Sensing of unexploded ordnance with magnetometer and induction data: Theory and signal processing," *IEEE Trans. Geosci. Remote Sens.*, vol. 41, pp. 1005–1015, 2003.

[14] K. Sun, K. O'Neill, F. Shubitidze, I. Shamatava, and K. D. Paulsen, "Fast data-

derived fundamental spheroidal excitation models with application to UXO discrimination," *IEEE Trans. Geosci. Remote Sens.*, vol. 43, pp. 2573–2583, 2005.

[15] J. P. Fernández, B. Barrowes, K. O'Neill, I. Shamatava, F. Shubitidze, and K. Sun, "A data-derived time-domain SEA for UXO identification using the MPV sensor," *Proc. SPIE*, vol. 6953, no. 6953-1H, 2008.

[16] F. Shubitidze, B. Barrowes, I. Shamatava, J. P. Fernández, and K. O'Neill, "Data-derived generalized SEA applied to MPV TD data," Applied Computational Electromagnetics Symposium, Niagara Falls, Mar.–Apr. 2008.

[17] I. Shamatava, F. Shubitidze, B. Barrowes, E. Demidenko, J. P. Fernández, and K. O'Neill, "The generalized SEA and a statistical signal processing approach applied to UXO discrimination," *Proc. SPIE*, vol. 6953, no. 6953-53, 2008.

[18] L.-P. Song, F. Shubitidze, L. R. Pasion, D. W. Oldenburg, and S. D. Billings, "Computing transient electromagnetic responses of a metallic object using a spheroidal excitation approach," *IEEE Geosci. Remote Sens. Lett.*, vol. 5, pp. 359–363, 2008.

[19] D. Marquardt, "An algorithm for least-squares estimation of non-linear parameters," *SIAM J. Appl. Math.*, vol. 11, pp. 431–441, 1963.

[20] I. Shamatava, F. Shubitidze, B. Barrowes, J. P. Fernández, L. R. Pasion, and K. O'Neill, "Applying the physically complete EMI models to the ESTCP Camp Sibert Pilot Study EM-63 data," *Proc. SPIE*, vol. 7303, no. 7303-23, 2009.

[21] F. Shubitidze, B. Barrowes, J. P. Fernández, I. Shamatava, and K. O'Neill, "APG UXO discrimination studies using advanced EMI models and TEMTADS data," *Proc. SPIE*, vol. 7303, no. 7303-21, 2009.

[22] I. Shamatava, F. Shubitidze, B. Barrowes, J. P. Fernández, and K. O'Neill, "Physically complete models applied to BUD time-domain EMI data," *Proc. SPIE*, vol. 7303, no. 7303-22, 2009.

Fridon Shubitidze received the degree of Diploma radio physicist (M.S.) from the Sukhumi branch of Tbilisi State University (TSU), Republic of Georgia, and the Cand.Sci. (Ph.D.) degree in radio physics (applied electromagnetics) from TSU. He has been a Member of the Laboratory of Applied Electrodynamics at TSU, a Postdoctoral Fellow with the National Technical University of Athens in Greece, and a Visiting Scientist at the University of British Columbia. He is currently a Research Professor with the Thayer School of Engineering, Dartmouth College, Hanover, NH. His current work focuses on numerical modeling of forward and inverse electromagnetic scattering by subsurface and underwater metallic objects and the electrodynamic aspects of DNA sequencing.

Juan Pablo Fernández received the degree of Físico from the Universidad de los Andes in Bogotá, Colombia, the Ph.D. degree in theoretical low-temperature physics from the University of Massachusetts Amherst, and the M.S. degree in engineering sciences from the Thayer School of Engineering, Dartmouth College, Hanover, NH, where he has also been a Research Associate. He has taught physics, mathematics, astronomy, Spanish, and scientific writing at universities in Colombia and the United States and has worked as a writer, editor, translator, and grant proposal review manager. His current research centers on the discrimination of unexploded ordnance using electromagnetic induction methods and machine learning.

Irma Shamatava received the degree of Diploma radio physicist (M.S.) from the Sukhumi branch of Tbilisi State University, Tbilisi, Georgia, where she was also part of the Computer Center staff and an Assistant Teacher of physics and mathematics. She is currently a Researcher with the Thayer School of Engineering, Dartmouth College, and with Sky Research, Inc., both in Hanover, NH. Her research interests focus on analytical and numerical modeling of electromagnetic scattering by subsurface metallic objects, especially unexploded ordnance.

Leonard R. Pasion studied mathematical physics at Simon Fraser University in British Columbia and received the M.Sc. and the Ph.D. degrees, both in geophysics, from the University of British Columbia in Vancouver, where he also was a Post Doctoral Fellow. At present he is Senior Scientist at Sky Research, Inc., in Vancouver, where he manages research programs focused on the detection and discrimination of UXO and landmines using geophysical data and conducts research on data processing techniques for UXO discrimination. He has been principal investigator in various projects funded by the Strategic Environmental Research and Development Program.

Benjamin E. Barrowes received both his B.S. and M.S. degrees in Electrical Engineering from Brigham Young University and the Ph.D. degree from the Massachusetts Institute of Technology. He was a Director's funded Postdoc at the Physics Division of the Los Alamos National Laboratory in New Mexico. Currently, he is a physicist with the ERDC Cold Regions Research and Engineering Laboratory in Hanover, NH. His research interests center on electromagnetic wave theory and modeling with applications including wind-wave interaction, electromagnetic scattering from the sea surface and from random media, nanoscale energy generation techniques, and electromagnetic induction models for nonspherical geometries. Other interests include automatic code conversion and translation and arbitrary precision computing.

Kevin O'Neill received the B.A. degree from Cornell University, Ithaca, NY, and the M.A., M.S.E., and Ph.D. degrees from Princeton University, Princeton, NJ. After a National Science Foundation Postdoctoral Fellowship at the Thayer School of Engineering at Dartmouth College and the U.S. Army Corps of Engineers Cold Regions Research and Engineering Laboratory (CRREL), both in Hanover, NH, he joined CRREL as a Research Civil Engineer and the Thayer School as an adjunct professor. He has been a Visiting Fellow in the Department of Agronomy, Cornell University, and a Visiting Scientist with the Center for Electromagnetic Theory and Applications at MIT. His current research centers on electromagnetic remote sensing of surfaces, layers, and especially buried objects such as unexploded ordnance.